Bivariate Decision Trees: Smaller, Interpretable, More Accurate

Rasul Kairgeldin
rkairgeldin@ucmerced.edu
University of California, Merced
Merced, CA, USA

Miguel Á. Carreira-Perpiñán
mcarreira-perpinan@ucmerced.edu
University of California, Merced
Merced, CA, USA

Abstract

Univariate decision trees, commonly used since the 1950s, predict by asking questions about a single feature in each decision node. While they are interpretable, they often lack competitive predictive accuracy due to their inability to model feature correlations. Multivariate (oblique) trees use multiple features in each node, capturing high-dimensional correlations better, but sometimes they can be difficult to interpret. We advocate for a model that strikes a useful middle ground: bivariate decision trees, which use two features in each node. This typically produces trees that not only are more accurate than univariate trees, but much smaller, which offsets the small increase in node complexity and keeps them interpretable. They also help data mining by constructing new features that are useful for discrimination, and by providing a form of supervised, hierarchical 2D visualization that reveals patterns such as clusters or linear structure. We give two new algorithms to learn bivariate trees: a fast one based on CART; and a slower one based on alternating optimization with a feature regularization term, which produces the best trees while still scaling to large datasets.

CCS Concepts

• **Computing methodologies** → **Classification and regression trees**.

Keywords

decision trees; interpretability; pairwise interactions

ACM Reference Format:
Rasul Kairgeldin and Miguel Á. Carreira-Perpiñán. 2024. Bivariate Decision Trees: Smaller, Interpretable, More Accurate. In *Proceedings of the 30th ACM SIGKDD Conference on Knowledge Discovery and Data Mining (KDD '24), August 25–29, 2024, Barcelona, Spain.* ACM, New York, NY, USA, 12 pages. https://doi.org/10.1145/3637528.3671903

1 Introduction

In many ways, decision trees stand alone in the statistical machine learning literature. They use conditional computation by design: an input instance follows a single root-leaf path, without using the rest of the tree parameters. Hence, inference time is extremely fast (logarithmic on the number of paths if the tree was complete). They handle the multiclass case directly, without the need for one-vs-all or one-vs-one approaches, as each leaf can be labeled with a particular class. And, although outside our scope in this paper, ensembles of trees are among the most powerful classifiers, at least for tabular data, while being far simpler to train and tune compared to neural networks. Finally, decision trees are perhaps most valued because of their interpretability, together with a handful of models (such as logistic regression, generalized additive models and scorecards). The way they achieve a prediction follows a sequence of simple questions about the input features which is quite close to human reasoning. A decision tree can be explained and audited at a global level by simple inspection. For a particular input instance, one can explain the tree prediction by following the corresponding root-leaf path, or solve a counterfactual explanation to find the minimal change to the input features that results in a desired prediction [7, 17]. Indeed, some applications of automated models are required to provide an explanation of their decision. A well-known example in the US are adverse actions by financial institutions (such as denial of a loan application), where "each applicant against whom adverse action is taken shall be entitled to a statement of reasons for such action from the creditor" (Equal Credit Opportunity Act, 1974). In cases like these, explainable models such as decision trees are essential.

The one serious disadvantage of decision trees is that they usually result in low predictive accuracy. There are two reasons for that. The first one is *a poor data model.* A typical decision tree is of the axis-aligned or univariate type, which means that each decision node or split operates on a single input feature (e.g. "if $x_7 > 10$ go right, otherwise go left"). When features are correlated, which is the usual situation in practice, this requires many zigzagging splits in order to construct an oblique decision boundary (i.e., a linear combination of features; see fig. 1). Thus, the resulting tree is big, which makes it harder to interpret, and will generalize poorly anyway. Another model shortcoming is that having each node examine only one feature limits the total number of features that can be examined along a path or on the whole tree. And the number of nodes in the tree is itself much smaller than the sample size, because a leaf cannot be empty of training instances. This can force the tree to ignore important features.

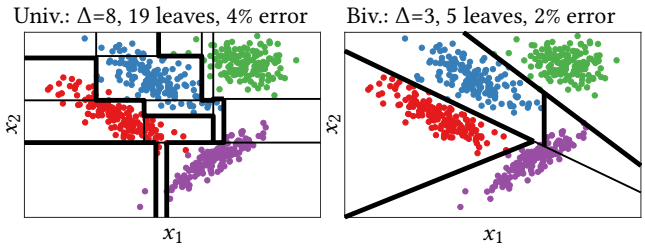

Figure 1: Partitioning by a univariate (left) and bivariate tree (right). By allowing some feature correlations, bivariate trees achieve better performance with much smaller trees.

KDD '24, August 25–29, 2024, Barcelona, Spain

ACM ISBN 979-8-4007-0490-1/24/08
https://doi.org/10.1145/3637528.3671903

The second reason is *a poor optimization*. The hard decisions that enable conditional computation in the tree also make it a piecewise constant function whose gradient with respect to its parameters is either zero or undefined. Optimizing a loss function over the tree is thus a very nonconvex problem. The most widespread way to train trees is the greedy recursive partitioning approach. Starting at the root, a node's split (feature and threshold) is fixed based on a local "purity" criterion, and the process is repeated recursively until a stopping criterion holds, possibly followed by a pruning procedure intended to reduce overfitting. CART [5] and C4.5 [31] are the foremost representative algorithms, differing on minor details (such as the choice of purity criterion). This approach does not optimize a global objective function over the tree (such as the 0/1 loss, cross-entropy or hinge loss), and indeed it results in quite suboptimal trees [19]. It does two things well, though: it is able to search for tree structures to some extent (itself a very difficult problem), and it is able to solve the local split problem exactly by enumerating all possible features and thresholds (the latter are the midpoints between scalar feature values). Indeed, CART and C4.5 remain in widespread practical use.

However, CART-like procedures were never successful for oblique (multivariate) trees, because the oblique split cannot be easily optimized by enumeration (indeed, it is NP-hard). While some approximations have been proposed (such as a local search [5, 25]), a suboptimal split has a cascade effect downstream that results in a big tree [19]. Since now each split uses all features, the tree is unwieldy and far from interpretable, which makes it not worth using even if some (often small) improvement occurs in the accuracy.

A recent algorithm, Tree Alternating Optimization (TAO) [8], has made it possible to train univariate and (sparse) oblique trees effectively. Unlike recursive partitioning, TAO operates on a well-defined parametric tree model and objective function. At each iteration, it updates each node's parameters so the objective decreases. It has been shown to produce univariate trees of higher accuracy than CART, C4.5 and other algorithms [38], and oblique trees that significantly exceed univariate trees in accuracy (as is to be expected, since they can directly model many-feature correlations) [8]. However, a univariate tree (even trained by TAO) is still a poor data model in many cases, while a (sparse) oblique tree can sometimes be hard to interpret if it uses many features in each node.

Our goal here is to design decision trees that are more accurate than univariate trees while remaining highly interpretable and efficient to train. We propose *bivariate trees*, where each decision node has zero, one or two features at most. Allowing for two features rather than one significantly increases the predictive accuracy and decreases the tree size even more significantly, improving interpretability, as shown in our experiments. This is made possible by our new algorithms to learn bivariate trees, of which we propose two: a very fast one, *bivariate CART*, based on greedy recursive partitioning, which can be conveniently implemented via a preprocessing step for univariate CART; and a slower but better one, *bivariate TAO*, based on alternating optimization. In the latter, we introduce a new regularization term that penalizes differentially the use of zero features (which makes the node redundant and results in automatically pruning the tree), one feature (univariate split) or two features (bivariate split); and we give a good, approximate but efficient solution to the bivariate split step that arises within TAO.

We believe bivariate trees strike a good tradeoff that can make them very practical. We explain their relation with pairwise-interaction models and other work in sections 2 and 3, and our training algorithms in section 4. Our experiments in section 5 compare univariate, bivariate and oblique trees in terms of accuracy, model size and interpretability.

2 Other pairwise-interaction models

Interpretable models based on pairwise interactions have a long history in machine learning, data mining and statistics. In fact, the idea of bivariate trees is not new (see related work), but it has never succeeded in practice, due to the lack of an effective optimization algorithm. We provide such algorithms in this paper and demonstrate how bivariate trees are indeed useful models.

Two widely used pairwise-interaction models are Generalized Additive Models with pairwise interactions (GA^2M) and Factorization Machines (FM). A GA^2M [18, sec. 9.5], [23] consists of a sum of univariate and bivariate component functions. A FM [32] is a low-rank bilinear model (the sum of linear and quadratic terms, where the latter's matrix is low-rank). These models are interpretable in that one can inspect the individual terms (e.g. with a 2D heatmap for each GA^2M pairwise term). The FM is especially useful with one-hot encoded categorical data, where each pairwise weight corresponds to the co-ocurrence of two categories.

In both cases, the total number of pairwise interactions with D features is $O(D^2)$, so it is critical to restrict the actual number of pairwise interactions. This is for interpretability but also to keep the number of parameters small, so the model can learn from limited sample sizes, often a problem in practice. In FMs this is achieved by using a matrix of rank $K < D$ for the quadratic term; in GA^2M, by greedily selecting a small subset of interactions. In bivariate trees, we control this by globally optimizing the loss plus a regularization term that penalizes the number of nodes, whose hyperparameter can be cross-validated or selected by hand to achieve a desired tree size. Note that, unlike FMs and GA^2Ms, bivariate trees are able to model more complex interactions due to the hierarchical structure of the tree (at the cost of making the tree deeper).

How interpretable are bivariate trees? On the one hand, each split involves now two features, so it is more complex. On the other hand, the ability to learn oblique splits (even with just two features) greatly reduces the number of nodes and depth of the tree compared to a univariate one, and hence the number of rules extracted from the tree. This can often make a bivariate tree *more interpretable* than a univariate one—a large univariate tree is not only complex, but examining it requires constant pan and zoom. A bivariate tree is also more accurate, particularly when the label depends on feature correlations. It can also happen that the bivariate split can be understood as a new, meaningful feature on its own right. Finally, bivariate trees bring another advantage over univariate trees: we can show a 2D scatterplot at each decision node on its two selected features, which behaves like a *hierarchical 2D linear discriminant analysis*. This shows information between-class (how specific classes are separated from each other), as well as within-class (such as clustering or linear structure). We convincingly demonstrate this our experiments by comparing bivariate and univariate trees in terms of accuracy and tree size, and by exploring in detail two case studies.

3 Related work

Learning trees has long been dominated by greedy recursive partitioning, of which countless versions exist [5, 22, 31, 33]. This has been more successful with univariate trees than oblique ones [5, 26], which are rarely used. Indeed, popular types of decision forests use univariate trees, such as random forests [4] or gradient boosting forests [10, 20]. Many implementations of univariate trees exist, from `scikit-learn` to commercial packages such as SAS, SPSS, Matlab or even Excel. Most univariate trees have a constant prediction at the leaves (class label or regression output), but there also exist more complex leaf models, such as linear [31], although, again, these are rarely used.

We have found only three papers exploring the idea of bivariate trees, all of them in the context of greedy recursive partitioning, differing in how they adapt the univariate split search to a bivariate one. Two early approaches [2, 24] used a variation of CART's local search for oblique splits. A recent one [3] used an exhaustive and expensive search for the bivariate split using branch-and-bound. Because of the underlying greedy recursive partitioning, this still results in large, suboptimal trees.

A parallel line of work on tree learning has focused on non-greedy approaches using exact, brute-force search. This has taken different forms: mixed-integer optimization [1, 34], dynamic programming in various forms [11] and other forms of combinatorial optimization [27, 28]. While cleverly designed, all these approaches have the fundamental disadvantage that their worst-case complexity is exponential on the problem size, so that they become infeasible for a nontrivial tree depth and number of nodes, or a nontrivial sample size or dimensionality. None of these approaches have considered bivariate splits.

A final line of work is the use of alternating optimization over the tree nodes, the TAO algorithm [8]. This has made it possible to optimize a given objective function over all the parameters of a fixed-structure tree, for tasks such as clustering [12], dimensionality reduction [36], semi-supervised learning [37] or imbalanced classification [15]. The resulting trees are smaller but more accurate than traditional ones [38], and similar advantages carry over to the forest setting [6, 9, 13, 14, 35]. Optimally updating a decision node given all other nodes (the reduced problem) takes the form of a certain 0/1 loss binary classification problem. This is NP-hard for oblique splits, but can be approximated by a surrogate loss, although this can often produce inadequate results. Here, we capitalize on the possibility to use partial enumeration in a 2D space of line orientations to find a good bivariate split efficiently.

Finally, it is possible to construct a bivariate tree by first applying feature selection to the problem to select two features globally and then fitting a tree. This gives a bivariate tree that uses the *same* two features in each node, which will result in a poor accuracy. We seek bivariate trees where each node can use *any* two features.

4 Learning bivariate trees

We consider classification (the extension to regression is straightforward and given later). Consider a K-class problem with dataset of size N with D-dimensional input features $\{(\mathbf{x}_n, y_n)\}_{n=1}^N \subset \mathbb{R}^D \times \{1, \dots, K\}$. Consider a binary decision tree (each decision node has exactly 2 children) with a set of decision nodes $\mathcal{N}_{\text{dec}}$, a set of leaves $\mathcal{N}_{\text{leaf}}$, and $\mathcal{N} = \mathcal{N}_{\text{dec}} \cup \mathcal{N}_{\text{leaf}}$. We define a routing function in each decision node $i \in \mathcal{N}_{\text{dec}}$ as $f_i(\mathbf{x}; \boldsymbol{\theta}_i)$: $\mathbb{R}^D \rightarrow \{\texttt{left}_i, \texttt{right}_i\} \subset \mathcal{N}$ which sends a sample $\mathbf{x}$ to either its left or right child. We use bivariate decision nodes where routing function makes hard decisions $f_i(\mathbf{x}; \boldsymbol{\theta}_i) = \texttt{left}_i$ if $w_{ij}x_j + w_{ik}x_k + b_i < 0$, otherwise $\texttt{right}_i$, and the learnable parameters are $\boldsymbol{\theta}_i = \{\mathbf{w}_i, b_i\}$, where $\|\mathbf{w}_i\|_0 \leq 2$ ensures splits of no more than 2 features. Each leaf $i \in \mathcal{N}_{\text{leaf}}$ contains a constant label classifier that outputs a single class $c_i \in \{1, \dots, K\}$. We collectively define the parameters of all nodes as $\boldsymbol{\Theta} = \{(\mathbf{w}_i, b_i)\}_{i \in \mathcal{N}_{\text{dec}}} \cup \{c_j\}_{j \in \mathcal{N}_{\text{leaf}}}$. The predictive function of the entire tree $T(\mathbf{x}; \boldsymbol{\Theta})$ guides a sample $\mathbf{x}$ along a single path from the root through a sequence of bivariate decision nodes to exactly one leaf, which provides the classification output.

We consider the following objective function over all the parameters of a tree of given structure, where $L(\cdot, \cdot)$ is the 0/1 loss:

$$E(\boldsymbol{\Theta}) = \sum_{n=1}^{N} L(y_n, T(\mathbf{x}_n; \boldsymbol{\Theta})) + \lambda \sum_{i \in \mathcal{N}_{\text{dec}}} \phi(\mathbf{w}_i) \quad \text{s.t.} \quad \begin{cases} \|\mathbf{w}_i\|_0 \leq 2, \\ i \in \mathcal{N}_{\text{dec}} \end{cases} \tag{1}$$

and we introduce the following, new type of regularization:

$$\phi(\mathbf{w}_i) = \begin{cases} C, & \text{if } \|\mathbf{w}_i\|_0 = 2 \\ \|\mathbf{w}_i\|_0, & \text{if } \|\mathbf{w}_i\|_0 < 2. \end{cases} \tag{2}$$

Both the ℓ_0 constraint and the penalty ϕ are different from the sparse oblique tree formulation of [8], which only had an ℓ_1 penalty; this does encourage oblique nodes with few features, but does not achieve bivariate nodes, as shown in our experiments. The *feature cost* regularization term (2) is critical in *allowing not just bivariate splits but also univariate ones and pruning nodes*. It imposes a cost of 0, 1 or C for each zero-, uni- or bivariate node (using 0, 1 or 2 features) in the tree, respectively. Using a cost $C > 1$ means bivariate splits are preferable to univariate ones only if they reduce the loss sufficiently. If a node uses no features ($\|\mathbf{w}_i\|_0 = 0$) then it sends all points either right or left (depending on b_i), so it is redundant and can be pruned at the end of the algorithm. Since using no features has cost zero, the regularization term in (1) counts the effective number of nodes in the tree (with a weight of 1 or C if using 1 or 2 features, resp.). Hence, the user can control the number of nodes in the tree via λ, and how uni- or bivariate the tree is via C.

4.1 The better algorithm: bivariate TAO

In equation (1), the loss function is additively separable over the training samples, and the regularization term is additively separable over the nodes. This renders it suitable for alternating optimization over the tree nodes (on a tree of given structure), which results in monotonic descent and convergence in a finite number of iterations. We follow an argument as in [8]. The idea is based on two theorems: separability condition and reduced problem (RP) over a node. First, define the *reduced set* $\mathcal{R}_i \subset \{1, \dots, N\}$ as the training instances that reach the node $i \in \mathcal{N}$. **Separability condition** implies that equation (1) can be separated and optimized over parameters of any non-descendant nodes (located on the same depth) independently and in parallel. This is a result of tree making hard decisions ($\mathcal{R}_i \cap \mathcal{R}_j = \emptyset$ for any non-descendant nodes i and j). **Reduced problem over a node** states that optimizing equation (1)

over parameters of the given node $i \in \mathcal{N}$ reduces to simpler, well-defined problem involving its reduced set $\mathcal{R}_i$. RP is different for decision nodes and leaves:

Leaf Equivalent to optimizing the top-level objective (1) over parameter c_i on $\mathcal{R}_i$. Exact solution: the majority class of the samples in $\mathcal{R}_i$: $c_i = \operatorname{argmax}_{k\in\{1,\dots,K\}} \sum_{n\in\mathcal{R}_i} L(y_n, k)$.

Decision node The objective (1) can be equivalently reduced to the following 0/1 *loss binary classification problem*:

$$E_i(\mathbf{w}_i, b_i) = \sum_{n\in\mathcal{R}_i} L(\bar{y}_n, f_i(\mathbf{x}_n; \mathbf{w}_i, b_i)) + \lambda\,\phi(\mathbf{w}_i) \text{ s.t. } \|\mathbf{w}_i\|_0 \le 2 \quad (3)$$

where L is the 0/1 loss and $\bar{y}_n \in \{\texttt{left}, \texttt{right}\}$ is a pseudolabel assigned to training instance x_n to indicate the child that yields a lower loss value. The loss is computed by propagating $\mathbf{x}_n$ down the corresponding child.

4.1.1 Solving the reduced problem over a decision node. Problem (3) arises with sparse oblique trees [8] and is NP-hard with arbitrary linear decision nodes, so there it is approximated via a surrogate loss. However, with the constraint $\|\mathbf{w}_i\|_0 \le 2$, the problem can be solved exactly in $O(N^3D^2)$ by enumerating every possible split (= linear dichotomy on the N instances) over all $\binom{D}{2}$ feature combinations. Unfortunately, this is very costly. We propose a faster, approximate solution which shows good results on practice.

Solution 1: L_{biv} (bivariate solution) of eq. (3) s.t. $\|\mathbf{w}_i\|_0 = 2$, $b_i \in \mathbb{R}$ is achieved at $\boldsymbol{\theta}_i^{\text{biv}} = \{\mathbf{w}_i^{\text{biv}}, b_i^{\text{biv}}\}$. Define a small, fixed subset of line orientations $\mathbf{W} \in \mathbb{R}^{2\times H}$ sampled uniformly in two dimensions by rotating it around the origin (H times) within a range of 0 to 180 degrees. For points in the reduced set $\mathcal{R}_i$ we select a pair of features and project them onto each orientation $\mathbf{w}_l \in \mathbf{W}$. It can be vectorized $\mathbf{X}_i^{\text{biv}} = \mathbf{X}_i\mathbf{S}\mathbf{W}$ where $\mathbf{X}_i \in \mathbb{R}^{|\mathcal{R}_i|\times D}$ is a matrix containing all instances in the reduced set $\mathcal{R}_i$, and $\mathbf{S} \in \mathbb{R}^{D\times 2}$ is a matrix with each column consisting of a 1 in the row corresponding to the selected feature and zeros everywhere else. Vectorization allows a GPU utilization for faster computation. The solution can be computed using thresholding over features of $\mathbf{X}_i^{\text{biv}}$. The resulting bias can be interpreted as an optimal split of the points projected onto selected orientation $\mathbf{w}_l$ to minimize number of misclassified instances in $\mathcal{R}_i$. We repeat this process for each pair of features and find best solution $\mathbf{w}_i^{\text{biv}}$, b_i^{biv}, where $\mathbf{w}_i^{\text{biv}}$ is a sparse vector. Pseudocode is in Fig. 3 and an illustration in Fig. 2.

Solution 2: L_{univ} (univariate solution) of eq. (3) s.t. $\|\mathbf{w}_i\|_0 = 1$, $b_i \in \mathbb{R}$ is achieved at $\boldsymbol{\theta}_i^{\text{univ}} = \{(0, w_i^{\text{univ}})^T, b_i^{\text{univ}}\}$. It is computed simply by thresholding over original features. For the decision node $i \in \mathcal{N}_{\text{dec}}$ algorithm selects one feature to split points in $\mathcal{R}_i$ in order to minimize eq. (3).

Solution 3: L_0 (zero-variate solution) of eq. (3) s.t. $\|\mathbf{w}_i\|_0 = 0$, $b_i \in \{-1, +1\}$ is achieved at $\boldsymbol{\theta}_i^0 = \{\mathbf{0}, b_i^0\}$. This indicates that all samples in $\mathcal{R}_i$ are sent to the left ($b_i^0 = -1$) or the right ($b_i^0 = 1$).

The solution of the RP can be summarized as follows:

$$\boldsymbol{\theta}_i^* = \begin{cases} \boldsymbol{\theta}_i^{\text{biv}}, & \text{if } L_{\text{biv}} + \lambda C < \min(L_{\text{univ}} + \lambda, L_0) \\ \boldsymbol{\theta}_i^{\text{univ}}, & \text{if } L_{\text{univ}} + \lambda < \min(L_{\text{biv}} + \lambda C, L_0) \\ \boldsymbol{\theta}_i^0, & \text{if } L_0 \le \min(L_{\text{biv}} + \lambda C, L_{\text{univ}} + \lambda) \end{cases}$$

We break the ties always in favor of a model with lower number of parameters. The separability condition allows us to optimize E in parallel for the parameters of any group of nodes that do not have a parent-child relationship, while keeping the parameters of the remaining nodes fixed. We optimize node parameters in the reverse breadth-first search order starting with deepest nodes and moving all the way to the root. This results in a monotonic decrease in the objective function E. It is important to note that after each iteration, the subset used for training each classifier or leaf predictor is modified. Some decision nodes will opt for not using a feature, hence being redundant (since it directs all input instances to the same child) and candidates for eventual removal in a postprocessing step at the end of the training. This means that bivariate TAO indeed achieves pruning, or equivalently learns the tree structure (subject to being a subset of the initial tree's structure).

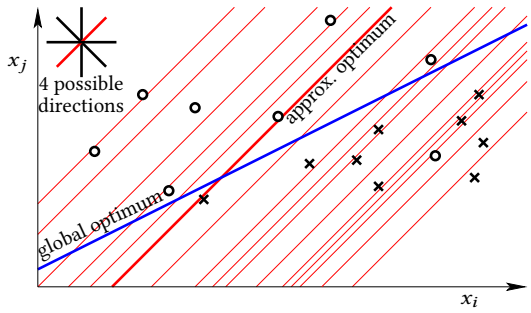

Figure 2: Illustration of our approximate solution of the reduced problem at a decision node assuming a selected pair of features (x_i, x_j). The instances in the reduced set of the node are labeled according to their pseudolabels (preferred child, left ∘ or right ×). The optimum (in 0/1 loss) linear classifier is the thick blue line (one misclassification). The approximate optimum found using the $H = 4$ possible directions (inset) is the thick red line (two misclassifications). The thin red lines are all the possible thresholds (passing through midpoints between projected instances) for the red orientation.

4.1.2 Regression. This requires just two modifications. First, the reduced problem over a leaf is solved by computing the mean of the samples in its reduced set. Second, the objective (1) in the decision node is now reduced to a weighted binary classification (instead of eq. (3)), where the weights are obtained by sending the sample down each child subtree and computing their respective loss.

4.1.3 Regularization path. For K-class classification problem with N training samples define $N_1 \ge N_2 \ge \cdots \ge N_K$, where N_1 is a number of samples in the most populous class. Considering that empty feature solution of the RP we can derive $\lambda\phi(\mathbf{w}_i) \ge L_0 - L_{\text{biv}} \in \{0, 1, \dots, N - N_1\}$. Since bivariate split generally produces lower 0/1 loss we typically set $C \ge 1$. Furthermore, considering that values of L are integer (number of misclassified points) it is enough to run the algorithm for $\lambda = \{0, 1, \dots, N - N_1\}$ to compute full regularization path. At $\lambda = N - N_1$ tree consists of a single leaf with the label of samples in N_1. We compute the full regularization path and select a tree with best validation error. Nodes with empty features are retained until the end of the algorithm since their solutions may become nonempty at later iterations or a larger λ.

In this context, $\lambda\phi(\mathbf{w}_i)$ can be interpreted as the maximum allowed number of misclassified samples by a decision node. When this threshold is exceeded, the node is pruned. For most datasets,

input training set $\{\mathbf{x}_n, y_n\}_{n=1}^N$,
binary axis-aligned tree T with given structure and
parameters $\boldsymbol{\Theta}$ at the nodes $\mathcal{N} = \mathcal{N}_{\text{dec}} \cup \mathcal{N}_{\text{leaf}}$
repeat
for $i \in \mathcal{N}$
$\mathcal{R}_i \leftarrow$ reduced set of node i
end if
for $d = \Delta$ **downto** 0 **do**
for $i \in$ nodes at depth d (can be done in parallel)
if $i \in \mathcal{N}_{\text{leaf}}$
$c_i \leftarrow$ majority class in $\mathcal{R}_i$
else
solution of reduced problem eq. (3) for decision node $i \in \mathcal{N}_{\text{dec}}$
end if
if $L_{\text{biv}} + \lambda C < \min(L_{\text{univ}} + \lambda, L_0)$
$\mathbf{w}_i, \mathbf{b}_i \leftarrow \boldsymbol{\theta}_i^{\text{biv}}$
else if $L_{\text{univ}} + \lambda < \min(L_{\text{biv}} + \lambda C, L_0)$
$\mathbf{w}_i, \mathbf{b}_i \leftarrow \boldsymbol{\theta}_i^{\text{univ}}$
else if $L_0 \leq \min(L_{\text{biv}} + \lambda C, L_{\text{univ}} + \lambda)$
$\mathbf{w}_i, \mathbf{b}_i \leftarrow \boldsymbol{\theta}_i^0$
end if
end for
end for
until $E(\boldsymbol{\Theta})$ does not strictly decrease
remove redundant nodes (empty features solution)
return trained T

input training set $\{\mathbf{x}_n, \bar{y}_n\}_{n \in \mathcal{R}_i}$ of decision node $i \in \mathcal{N}_{\text{dec}}$,
matrix of orientations $\mathbf{W} \in \mathbb{R}^{2 \times H}$
for each pair of features $j, k \in D$
for $\mathbf{w}_l \in \mathbf{W}$
$\mathbf{x}_l^{j,k} \leftarrow$ project selected features of
each sample in $\mathcal{R}_i$ onto $\mathbf{w}_l$
$b_l^{j,k} \leftarrow$ optimal thresholding over $\mathbf{x}_l^{j,k}$
if $j, k, \mathbf{w}_l, b_l^{j,k}$ produce lowest value of eq. (3)
$\boldsymbol{\theta}_i^{biv} \leftarrow \{\mathbf{w}^*, b_l^{j,k}\}$, where $\mathbf{w}^*$ is a sparse vector
of all zeros with corresponding value of $\mathbf{w}_l$
at j, k
end if
end for
end for
return θ_i^{biv}

Figure 3: Pseudocode: bivariate TAO algorithm (top); solution to the reduced problem in a decision node i (bottom).

there exists a range of λ values where tree parameters does not change. Knowing the minimum difference in 0/1 loss between empty feature solution and current best solution (univariate or bivariate) for each decision node we can calculate next significant λ in regularization path. This way full regularization path can be computed much faster.

4.1.4 Computational complexity. Assume N training samples and a complete tree of depth Δ (having $2^\Delta - 1$ decision nodes). Call $\mathcal{R}_i$ the reduced set of node i. At the start of each iteration we update $\mathcal{R}_i$ for each node by propagating each training instance to its corresponding leaf, which is $O(\Delta N)$ with space complexity of $O(N)$ to store indices.

We optimize node parameters in reverse BFS order starting with leaves. For each leaf $i \in \mathcal{N}_{\text{leaf}}$ we compute label using majority vote in $O(|\mathcal{R}_i|)$. For each decision node $i \in \mathcal{N}_{\text{dec}}$ we first compute pseudolabels by sending samples of reduces set to the left and right child at $O(2\Delta|\mathcal{R}_i|)$. For univariate split, we sort instance feature values $\{x_{nd}\}_{n \in \mathcal{R}_i}$ before thresholding. In the final step, we determine the loss for every bias value similar to how the purest split is computed within recursive partitioning. It can be done exactly and efficiently through an incremental method, where we calculate the loss for the next bias value based on the loss of the current value. The total computational complexity for D features is $O(D\Delta|\mathcal{R}_i|) + \Theta(D|\mathcal{R}_i| \log |\mathcal{R}_i|)$. For bivariate split the process is computationally similar to finding univariate split on $\mathbf{X}_i^{biv}$ (described in 4.1) for every pair of features. Since H is constant, total computations complexity is $O(D^2\Delta|\mathcal{R}_i|^2) + \Theta(D^2|\mathcal{R}_i|^2 \log |\mathcal{R}_i|)$.

The total cost of training is dominated by decision nodes. At any depth the union of all reduced sets is the whole training set. In this case the total computational cost is upper bounded by $\Theta(\Delta^2 D^2 N^2 + \Delta D^2 N^2 \log N)$. It is worth mentioning that decision nodes at each depth can be trained in parallel, which drastically reduces running time of the algorithm.

4.2 The faster algorithm: bivariate CART

Our idea above of partial enumeration over the bivariate splits can be combined with greedy recursive partitioning (in particular CART). This does not anymore optimize any global objective function and it produces worse trees than bivariate TAO, but it is much faster. It can be done in two ways. One, more efficient, is by modifying the CART split step (based on the Gini index) to use the partial enumeration, in a similar way to the TAO decision node reduced problem above. Another, less efficient (in memory), is to construct a new, augmented training set with $\leq D + \binom{D}{2}|H|$ features in advance and simply run the usual, univariate CART on it. This algorithm works quite well, as seen in our experiments, resulting in bivariate trees that are quite smaller and generalize better than univariate CART. Note this algorithm is different from previous work on bivariate trees.

4.3 Interaction of C and λ: a phase diagram

Here we give a qualitative understanding of the effect of the feature cost C and the regularization hyperparameter λ on the size of the tree and the number of features it uses. It can be plotted as a "phase diagram" in (λ, C)-space such as that in fig. 4. Inspection of the objective function shows that, since the loss is always less than N (where N is the sample size), there exists a critical value $0 < \lambda^* < N$ such that the optimal tree for $\lambda \geq \lambda^*$ consists of a single leaf node with a constant label (zero-variate tree). Likewise, for small enough λ, all nodes are bivariate if $C \leq 1$ (since univariate splits are no cheaper and less powerful); and there exists a critical value $1 < C^* \leq N$ such that all nodes are univariate if $C \geq C^*$ (since even a single bivariate node is too costly). Trees with both uni- and bivariate nodes exist for a region $(0, \lambda^*] \times (1, C^*]$, which contains the practically useful models, where we allow the objective function to determine the optimal uni/bivariate ratio. This also suggests a simplified training strategy where we fix C to a value a bit over one (on practice, $C \in [1.1, 1.5]$) and cross-validate λ.

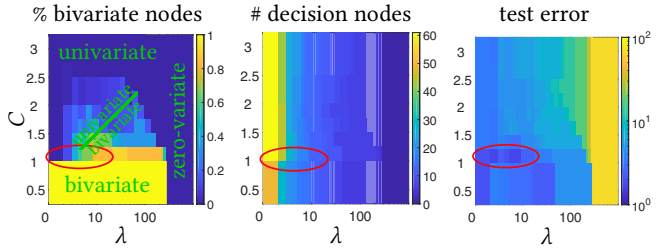

Figure 4: Phase diagram (λ, C) for the Segment dataset. We plot: the proportion of bivariate vs univariate decision nodes (indicating the regions of pure zero-, uni- and bivariate trees); the number of decision nodes; and the test error (%). The ellipse indicates the region of best-error trees.

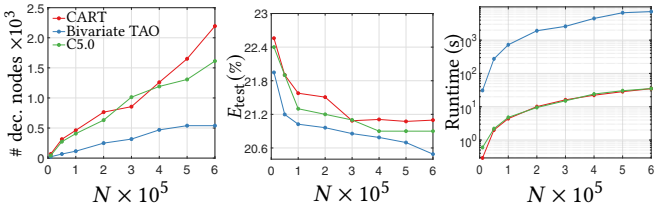

Figure 5: Number of nodes, test error and training time for univariate CART and C5.0 and bivariate TAO trees as a function of the sample size (subsampled from the SUSY dataset).

5 Experiments

We provide all necessary details about hyperparameters, implementations of different algorithms, etc. in the appendix.

Accuracy, tree size and number of features. Table 1 shows that, almost without exception across several datasets of varying types, our bivariate TAO tree is both most accurate and smallest compared to any other univariate tree (CART [5], C5.0 [31]) or bivariate tree (in particular, BiDT [3]). This is as expected: it uses the more flexible model and the better optimization. Next best is our other, more approximate algorithm, bivariate CART. The improvement in accuracy over univariate trees is consistent and varies depending on the dataset (usually a few percentage points). *The reduction in depth and number of nodes, and the corresponding simplification of the tree, is drastic, typically several times fewer nodes* (17 times smaller on the MiniBooNE dataset). In terms of training time, although not as lightning-fast as univariate trees, our bivariate trees scale well to large datasets (unlike BiDT, which times out, as expected from its brute-force search). When compared with the oblique trees, bivariate TAO trees are less accurate (as expected) but there is often little difference. However, oblique trees use quite a lot of features per node, which makes them more complex. Similar conclusions follow from the results for regression (table 2).

Dependence on sample size. It is well known that univariate trees (CART, C5.0) grow in size proportionally to the sample size, indicating a suboptimal training and pruning, as a consequence of their greedy recursive partitioning [29]. This is confirmed in fig. 5, where they continue to grow even when their accuracy plateaus after reaching ≈50% of the total. In contrast, our bivariate TAO tree slowly grows in size but eventually stops, indicating it has reached

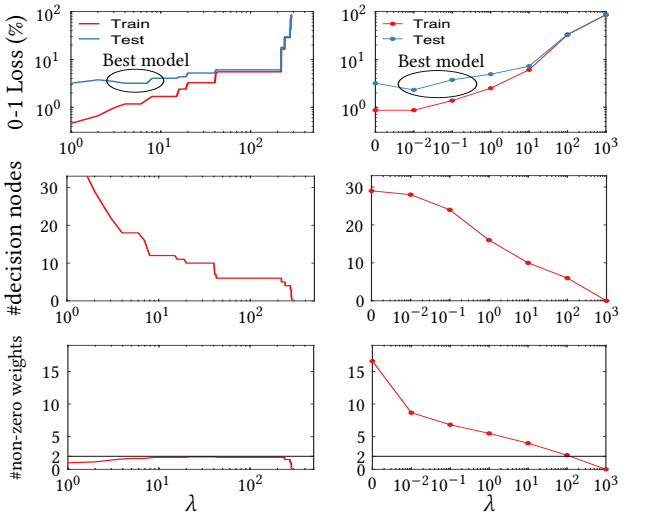

Figure 6: 0/1 loss, number of nodes and average number of features per decision node for bivariate (left) and oblique trees (right) over their regularization path (Segment dataset).

a sufficient model size—all the while with a better accuracy and much smaller size (≈3–5 times) than the univariate trees. With our unoptimized code, bivariate TAO is much slower to train than the (extremely fast) CART and C5.0, but it is still good for practical use.

Oblique trees use many features. Here we show that one cannot achieve a bivariate tree by overpenalizing a sparse oblique tree. The latter, proposed in [8], minimizes the sum of the 0/1 loss plus an ℓ_1 penalty $\lambda \sum_i \|\mathbf{w}_i\|_1$ on the weight vector of each decision node i in the tree, with hyperparameter $\lambda \geq 0$. Fig. 6 shows the entire regularization path for a sparse oblique tree and a bivariate tree on the Segment dataset. While the bivariate tree has an average of at most 2 features per node throughout its path, the oblique one reaches an average of 2 only for very high λ, at which point the tree is very small and has an enormous error. The reason for this is that, while increasing λ does encourage sparsity of weight vectors over the whole tree, this sparsity results in some nodes being pruned (whenever $\mathbf{w}_i = \mathbf{0}$) while other nodes use more features. In this dataset, the best trees have about the same error (≈2.5%) and number of nodes (≈16) for both bivariate and oblique, but the latter using ≈7 features per node.

5.1 Interpretability of bivariate trees

The small size of a (well-optimized) bivariate tree and the ability to visualize its decision nodes makes it highly interpretable, as we demonstrate here in two examples.

5.1.1 Breast Cancer UCI dataset. This is a binary classification task into malignant and bening tumors. Each input instance contains 30 features (listed in appendix table 4) extracted from a collection of cells, specifically, geometric features about size, shape, etc. (measured from snake-generated cell nuclei boundaries). Each such feature is very informative on its own and can be readily identified and understood by a radiologist.

Table 1: Comparison between bivariate, univariate and oblique trees for classification. Each tree was selected by cross-validating its hyperparameter and this was repeated 3 times over random training/validation sets. We report training and test accuracy (% ±stdev); average depth Δ, node count n and number of features f per node (we omit $f = 1$ and 2 for univariate and bivariate trees, respectively); and average runtime (seconds or "timeout"). We indicate with color green best and blue second best result for test accuracy and node count over the univariate and bivariate trees (ignoring the oblique trees).

Dataset	(N_{train}, D, K)		bivariate TAO	bivariate CART	bivariate BiDT	univariate CART	univariate C5.0	oblique TAO
Breast Cancer	(455,30, 2)	training (%)	96.04±1.53	99.12±0.00	96.99±0.10	98.61±0.41	98.9±0.48	98.21±0.79
		test (%)	98.25±0.43	98.00±0.00	97.66±0.10	94.73±0.00	95.6±0.67	97.71±1.04
		Δ/#nodes/f	1/3	3.0/9	1.6/5	4.0/16	5.3/12	3/15/10.3
		runtime (s)	4	6	2	0.1	0.1	5
Segment	(1963,19, 7)	training (%)	98.47±0.35	97.30±0.00	97.58±0.01	98.76±0.00	98.9±0.10	99.48±0.21
		test (%)	97.41±0.14	96.73±0.14	96.06±0.14	96.01±0.47	96.3±0.48	97.58±1.31
		Δ/#nodes/f	11.0/13	11.0/25	9.0/21	15.0/128	12.25/77	8/271/8.5
		runtime (s)	30	13	27	0.1	0.1	20
Spambase	(3910,57, 2)	training (%)	96.39±0.08	97.49±0.14	95.34±1.85	97.86±2.91	96.16±0.14	96.55±0.47
		test (%)	93.34±0.07	92.19±0.05	92.71±0.53	92.18±0.31	92.2±0.42	94.31±1.22
		Δ/#nodes/f	14/53	10.0/77	16/161	24.7/362	14.7/77	4/30/42.1
		runtime (s)	120	284	208	0.3	0.3	60
House 16H	(11464,16, 2)	training (%)	87.1±1.55	89.45±0.00	90.42±0.23	86.2±0.0	91.98±0.55	86.55±1.10
		test (%)	85.6±0.07	84.73±0.05	85.6±0.17	83.4±0.0	83.06±0.32	85.47±0.51
		Δ/#nodes/f	7/35	10/107	10/115	8/75	15.05/245	4/13/14.9
		runtime (s)	30	21	15	0.2	0.1	24
Letter	(16000,16,26)	training (%)	100±1.37	100±0.01	98.40±1.76	94.30±0.01	98.66±0.07	95.43±0.29
		test (%)	87.25±0.11	87.25±0.00	86.80±0.37	86.04±0.04	86.76±0.33	90.41±0.31
		Δ/#nodes/f	35/1314	35.0/2121	37.6/2596	28/3888	16.85/2817	11/2155/8.5
		runtime (s)	300	73	12	0.3	0.9	77
Electricity	(32702, 8, 2)	training (%)	98.97±2.80	95.80±0.80	96.14±1.20	99.10±0.00	95.04±0.43	98.1±1.8
		test (%)	89.38±0.12	86.05±0.05	87.91±0.06	87.80±0.16	88.64±0.42	90.23±0.19
		Δ/#nodes/f	23.0/1083	24.0/1741	22.3/1881	30.0/6366	17.25/2615	10/249/6.8
		runtime (s)	300	81	393	0.9	0.9	134
MiniBooNE	(62048,50, 2)	training (%)	92.36±0.00	96.02±0.02	-	96.61±0.02	95.88±0.07	91.98±0.15
		test (%)	91.16±0.00	90.68±0.03	-	90.25±0.03	89.84±0.10	91.43±0.12
		Δ/#nodes/f	11.0/105	15/831	-	19.3/2012	15.65/1787	10/133/16.8
		runtime (s)	1200	1000	timeout	5.2	6.4	3000
SUSY	(600000,18, 2)	training (%)	80.71±0.00	81.35±0.00	-	81.45±0.00	80.90±0.00	81.10±0.00
		test (%)	79.51±0.00	79.01±0.00	-	78.90±0.00	79.10±0.00	80.3±0.00
		Δ/#nodes/f	17.0/1077	21/2780	-	24/4389	16.25/3227	12/983
		runtime (s)	≈2h	≈1h	timeout	40.2	35.2	≈2h

Table 2: Like table 1 but for regression, reporting RMSE ±stdev over 3 runs.

Dataset	(N_{train}, D, K)	bivariate TAO	bivariate CART	univariate CART	oblique TAO
airfoil	(1002, 5, 1)	0.34±0.13	0.01±0.00	0.52±0.10	3.02±0.29
		2.46±0.43	2.72±0.02	2.75±0.62	3.13±0.38
		16/252	22/2133	15/479	8/147/3
		15	5	1.3	13
abalone	(2506, 8, 1)	2.14±0.03	0.39±0.12	2.32±0.11	2.11±0.02
		2.24±0.13	2.95±0.38	2.34±0.59	2.18±0.05
		2/7	23/903	7/39	6/58.6/6
		21	10	0.9	19
cpuact	(4915,21, 1)	1.84±0.53	1.74±0.43	2.10±0.71	2.47±0.07
		3.11±0.10	3.33±0.31	3.97±1.32	2.71±0.04
		10/191	14/327	13/373	6/52.7/13
		27	17	1.3	13
ailerons	(7154,40, 1)	1.88±0.03	0.71±0.00	1.81±0.12	1.65±0.02
		2.03±0.00	2.21±0.00	2.25±0.63	1.76±0.05
		5/21	15/50	21/105	6/60.2/13
		27	20	1.3	21

Fig. 9 (appendix) shows how our bivariate TAO trees dominate the univariate CART trees by a significant margin over the range of tree sizes. Fig. 7 shows the best trees in terms of cross-validation. The univariate CART tree has depth 7, 16 leaves and 6.4% error. The bivariate TAO tree has depth 3, 5 leaves and 2% error. Not only is the bivariate much more accurate, but its small size makes it easier to understand by simple inspection. It results in only 5 rules vs 16 rules for the univariate tree.

Global level structure. The tree structure shows the bivariate tree can represent the whole dataset only in 5 very simple IF-THEN-ELSE rules. It is notable that the tree performs a significant feature selection. It uses only 6 features (out of 30). Three of them concern the *radius* measurements of nuclei boundaries (mean value, largest value and standard error), and obviously capture *size* information about the cells. Two of them concern *contour concavities* (mean value and standard error), and obviously capture *shape* information about the cells (essentially, whether they are circle-like or have indentations). The last feature is the texture (mean value) of the cell nuclei. The tree ignores features about smoothness of the contour, area of the cells, perimeter of the cell contour, fractal

univariate CART tree: $\Delta = 7$, 16 leaves, $E_{\text{test}} = 6.4\%$

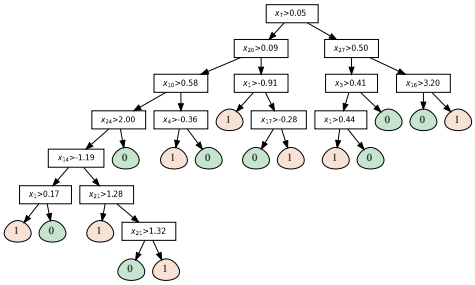

1: **if** $(x_7 > 0.05)$ & $(x_{20} > 0.09)$ & $(x_{10} > 0.58)$ & $(x_{24} > 2.00)$ & $(x_{14} > -1.19)$ & $(x_1 > 0.17)$ **then** PREDICT 1 **end if**
2: **if** $(x_7 > 0.05)$ & $(x_{20} > 0.09)$ & $(x_{10} > 0.58)$ & $(x_{24} > 2.00)$ & $(x_{14} > -1.19)$ & $(x_1 \leq 0.17)$ **then** PREDICT 0 **end if**
3: **if** $(x_7 \leq 0.05)$ & $(x_{27} \leq 0.50)$ & $(x_{16} \leq 3.20)$ **then** PREDICT 1 **end if**
4: **if** $(x_7 \leq 0.05)$ & $(x_{27} \leq 0.50)$ & $(x_{16} > 3.20)$ **then** PREDICT 0 **end if**
5: ...//**12 MORE RULES**...

bivariate TAO tree: $\Delta = 3$, 5 leaves, $E_{\text{test}} = 2.0\%$

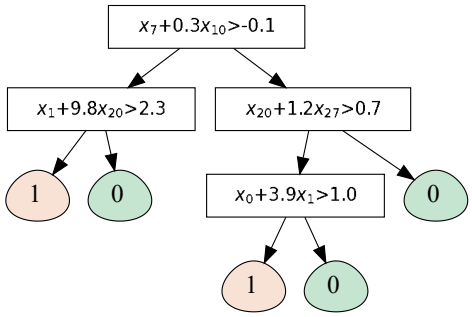

1: **if** $(x_7 + 0.3x_{10} > -0.1)$ & $(x_1 + 9.8x_{20} > 2.3)$ **then** PREDICT 1 **end if**
2: **if** $(x_7 + 0.3x_{10} > -0.1)$ & $(x_1 + 9.8x_{20} \leq 2.3)$ **then** PREDICT 0 **end if**
3: **if** $(x_7 + 0.3x_{10} \leq -0.1)$ & $(x_{20} + 1.2x_{27} \leq 0.7)$ **then** PREDICT 0 **end if**
4: **if** $(x_7 + 0.3x_{10} \leq -0.1)$ & $(x_{20} + 1.2x_{27} > 0.7)$ & $(x_0 + 3.9x_1 > 1.0)$ **then** PREDICT 1
5: **else** PREDICT 0 **end if**

Figure 7: Best univariate CART tree and bivariate TAO tree with their sets of rules (Breast Cancer dataset).

dimension, etc. This makes sense since some of those are likely correlated with size and shape as given by the radius and concavity, and thus are redundant.

Local level structure. At a local level in the tree, we can look at specific nodes. The pairwise combination of features learned in each decision node can be seen as a new, constructed feature, which is quite meaningful and further improves interpretability. For example, the root of the tree (which uses as features the largest cell radius and the mean concavity) can be understood as detecting a cell collection where the cell nuclei boundaries are irregular or unusually large. The root's right child uses as features the standard error of radius and concavity, which means it detects high variance in the shape and size of the cell collection (as opposed to a collection that has uniform shape and size). Taking these two nodes together, the tree predicts malignancy (rightmost path). This can be done with the other 4 leaves, each of which is a population (malignant or benign) characterized by a short path or rule involving very few constructed features that are meaningful. As another example, the deepest decision node classifies the cell collection as malignant based on a combination of average size and texture variance irregularities.

5.1.2 Segment dataset. Consider now fig. 8, which shows a bivariate TAO tree on the Segment dataset, a standard UCI benchmark for classification. It has 1963 instances training, 19 continuous features and 7 classes (balanced). Each class is an original color image and each feature is a local descriptor based on 3×3 patches (listed in the appendix, table 5). The bivariate tree has 25 nodes (12 decision nodes, 13 leaves), depth 10, and a training and test error of 1.53% and 2.59%, respectively. The univariate CART tree with lowest test error (not shown) is much bigger: 128 nodes, depth 15 and test error 3.99%. If we tune CART post-pruning to achieve 25 nodes, the error increases to 7.5%. Inspecting the bivariate tree reveals a wealth of information about the data, as we discuss next. Such insight would not be possible with black-box models such as forests or neural nets.

Global level structure. The tree is heavily lopsided, having depth 10 but only 13 leaves. This means for most decision nodes one or both children is a leaf, so the IF-THEN-ELSE rules corresponding to the tree are almost perfectly tail-recursive. This makes them more interpretable, and faster at inference (many leaves have low depth).

A consequence of the lopsided structure is that several classes, accounting for over 50% of the dataset, are processed in a cascade way, and the tree makes early decisions for them (with very short rules). For example, class 3 is decided at the root (node A) after a single bivariate decision, with zero training error. Classes 5, 4 and 0 are also decided in a single root-leaf path each after 2, 3 and 5 decision nodes (one of them univariate), respectively, with near-zero training error. Classes 1, 2 and 6 are harder to separate and require deeper rules.

The tree has performed a significant *feature selection*: it uses only 10 features (0 1 5 6 7 9 10 12 15 18) out of the total 19. Since the tree has 12 decision nodes, it could use up to 24 distinct features, but it uses fewer. This is driven by the optimization we apply, which globally updates all the tree parameters. In contrast, a univariate tree with 12 decision nodes would be forced to use at most 12 features no matter what, because it can have only one in each node. In order to use sufficiently many features, a univariate tree has to be overly deep, which limits their interpretability.

Local level structure. We show a scatterplot at each decision node projecting the instances reaching it onto its two features and showing the boundary of the split. The scatterplots show the power of bivariate splits (most obviously in nodes E, G, J, etc.). Using univariate splits would require a deep sequence of splits. More importantly, *the scatterplots provide a form of supervised dimensionality reduction, like a linear discriminant analysis but tree-structured, which is very helpful for visualization.* It is also directly interpretable because the projection is directly on two original features (rather than a complex function of all the features). For example, nodes C and E show a distinct cluster structure in classes 4 and 0, respectively. Although we were not able to obtain original images of Segment dataset, we conjecture that these clusters might correspond

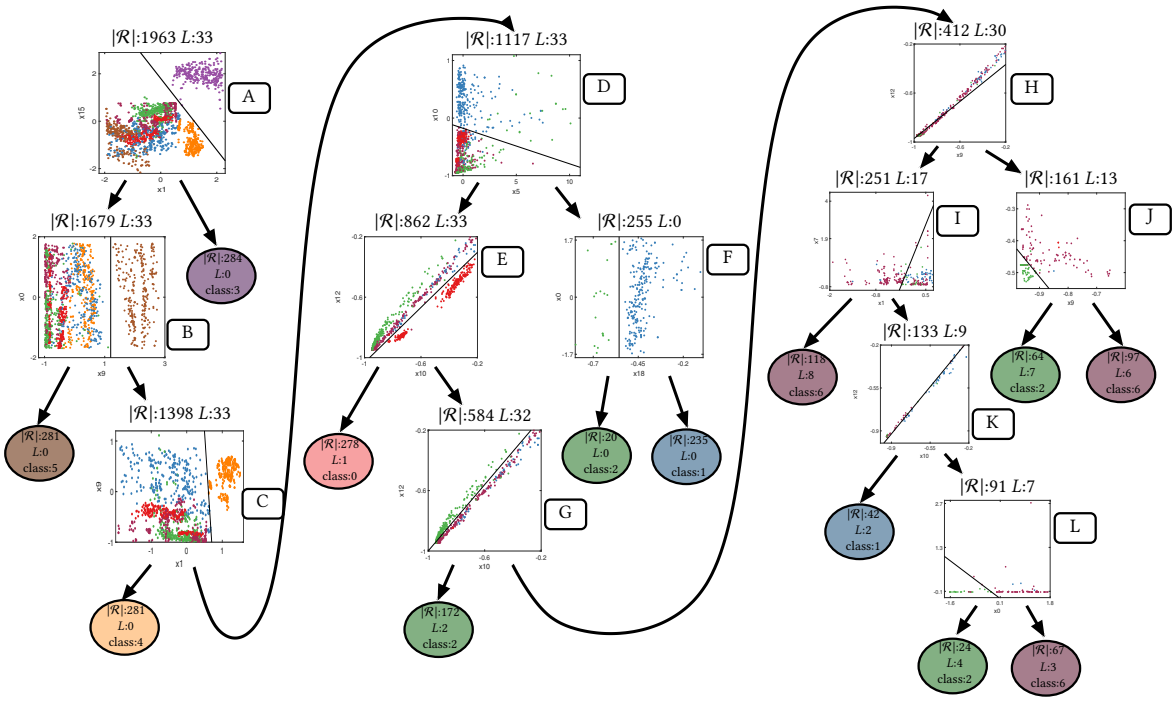

Figure 8: A bivariate TAO tree on the Segment dataset, plotted in 3 columns so it fits. Each decision node shows a scatterplot of its instances onto its two features. Each node shows the number of training instances reaching it ($|\mathcal{R}|$ and their 0/1 loss (L).

to objects of different color. Nodes E, G and K all use a bivariate split on features (10,12) and show a clear linear, parallel structure over multiple classes. Features 10 and 12 correspond to average amount of red and green color of the region. Bivariate split can be interpreted as a mixture of these two colors. Samples of class 0 in node E can be separated from other samples by measuring the amount of this mixture and thresholding it using bias.

All nodes use bivariate splits except nodes B and F, which use a univariate split. For plotting purposes only (so we can show a 2D scatterplot), we include feature 0 (region centroid column) as the vertical axis in those nodes. This has the serendipitous effect of showing that all classes show a linear structure along feature 0.

Note how some bivariate splits are able to separate out one class from the others cleanly (e.g. nodes A, B, C and E). But, in general, this is not possible with a linear decision boundary and it requires further partitioning down the tree. For example, nodes D and E show a sequence of two splits that separate class 0 from the rest. Thus, we should generally expect that a given decision node will have some classes straddling both sides of the boundary.

The bivariate decision functions can usually be understood as new, meaningful features. For example, split in node D can be interpreted as a combination of average amount of red color in the region and a contrast of adjacent pixels. We assume it can help to distinguish presence of vertical edges of specific color tone. Some features are repeatedly used (sometimes the same pair of features), indicating their relevance to separating some group of classes. For example, features 1 (row of the center pixel of the region) and 9 (average intensity of the region) are critical to separate cleanly first class 3 and then class 4 from the rest. This make sense since it indicates position of the 3 by 3 patch and its color the intensity. Some features are used only once, deep down the tree and affecting a small subset of instances, indicating they are needed to make a fine distinction. For example, features 0 and 6 appear only once and together in the deepest node (L). Some bivariate splits could be turned into univariate ones (eg nodes A and C) but at a higher loss. For example making univariate split at node A results in 15 more misclassified points.

6 Conclusion

We have proposed bivariate decision trees as a practically useful tradeoff between univariate trees and oblique trees. They are highly interpretable because they use two features at most in each decision node, unlike oblique trees, which use all or many features. Compared to univariate trees, bivariate trees are much smaller but significantly more accurate. They also can reveal insights about the data by constructing new, bivariate features that are useful for discrimination; and by providing a form of supervised, hierarchical 2D visualization at each decision node, which reveals patterns in the data such as clusters or linear structure. To learn a bivariate tree, we have given two algorithms. One is very fast, based on greedy recursive partitioning. The other is slower but produces much better trees, by using alternating optimization of the loss and the node features' cost globally over all the tree parameters.

Acknowledgments. Work supported by NSF award IIS–2007147. We thank M. Gabidolla for help with the TAO implementation.

References

[1] Dimitris Bertsimas and Jack Dunn. 2017. Optimal Classification Trees. *Machine Learning* 106, 7 (July 2017), 1039–1082.

[2] Jan C. Bioch, Onno van der Meer, and Rob Potharst. 1997. Bivariate Decision Trees. In *Proc. European Symposium on Principles of Data Mining and Knowledge Discovery (PKDD 1997)*, J. Komorowski and J. Zytkow (Eds.). 232–242.

[3] Ferdinand Bollwein and Stephan Westphal. 2021. A Branch & Bound Algorithm To Determine Optimal Bivariate Splits for Oblique Decision Tree Induction. *Applied Intelligence* 51, 10 (Oct. 2021), 7552–7572.

[4] Leo Breiman. 2001. Random Forests. *Machine Learning* 45, 1 (Oct. 2001), 5–32.

[5] Leo J. Breiman, Jerome H. Friedman, R. A. Olshen, and Charles J. Stone. 1984. *Classification and Regression Trees.* Wadsworth, Belmont, Calif.

[6] Miguel Á. Carreira-Perpiñán, Magzhan Gabidolla, and Arman Zharmagambetov. 2023. Towards Better Decision Forests: Forest Alternating Optimization. In *Proc. of the 2023 IEEE Computer Society Conf. Computer Vision and Pattern Recognition (CVPR'23)*. Vancouver, Canada, 7589–7598.

[7] Miguel Á. Carreira-Perpiñán and Suryabhan Singh Hada. 2021. Counterfactual Explanations for Oblique Decision Trees: Exact, Efficient Algorithms. In *Proc. of the 35th AAAI Conference on Artificial Intelligence (AAAI 2021)*. Online, 6903–6911.

[8] Miguel Á. Carreira-Perpiñán and Pooya Tavallali. 2018. Alternating Optimization of Decision Trees, with Application to Learning Sparse Oblique Trees. In *Advances in Neural Information Processing Systems (NEURIPS)*, S. Bengio, H. Wallach, H. Larochelle, K. Grauman, N. Cesa-Bianchi, and R. Garnett (Eds.), Vol. 31. MIT Press, Cambridge, MA, 1211–1221.

[9] Miguel Á. Carreira-Perpiñán and Arman Zharmagambetov. 2020. Ensembles of Bagged TAO Trees Consistently Improve over Random Forests, AdaBoost and Gradient Boosting. In *Proc. of the 2020 ACM-IMS Foundations of Data Science Conference (FODS 2020)*. Seattle, WA, 35–46.

[10] Tianqi Chen and Carlos Guestrin. 2016. XGBoost: A Scalable Tree Boosting System. In *Proc. of the 22nd ACM SIGKDD Int. Conf. Knowledge Discovery and Data Mining (SIGKDD 2016)*. San Francisco, CA, 785–794.

[11] Emir Demirović, Anna Lukina, Emmanuel Hebrard, Jeffrey Chan, James Bailey, Christopher Leckie, Kotagiri Ramamohanarao, and Peter J. Stuckey. 2022. MurTree: Optimal Decision Trees via Dynamic Programming and Search. *J. Machine Learning Research* 23, 26 (2022), 1–47.

[12] Magzhan Gabidolla and Miguel Á. Carreira-Perpiñán. 2022. Optimal Interpretable Clustering Using Oblique Decision Trees. In *Proc. of the 28th ACM SIGKDD Int. Conf. Knowledge Discovery and Data Mining (SIGKDD 2022)*. Washington, DC, 400–410.

[13] Magzhan Gabidolla and Miguel Á. Carreira-Perpiñán. 2022. Pushing the Envelope of Gradient Boosting Forests via Globally-Optimized Oblique Trees. In *Proc. of the 2022 IEEE Computer Society Conf. Computer Vision and Pattern Recognition (CVPR'22)*. New Orleans, LA, 285–294.

[14] Magzhan Gabidolla, Arman Zharmagambetov, and Miguel Á. Carreira-Perpiñán. 2022. Improved Multiclass AdaBoost Using Sparse Oblique Decision Trees. In *Int. J. Conf. Neural Networks (IJCNN'22)*. Padua, Italy.

[15] Magzhan Gabidolla, Arman Zharmagambetov, and Miguel Á. Carreira-Perpiñán. 2024. Beyond the ROC Curve: Classification Trees Using Cost-Optimal Curves, with Application to Imbalanced Datasets. In *Proc. of the 41th Int. Conf. Machine Learning (ICML 2024)*. Vienna, Austria.

[16] Léo Grinsztajn, Edouard Oyallon, and Gaël Varoquaux. 2022. Why Do Tree-Based Models Still Outperform Deep Learning on Tabular Data?. In *Advances in Neural Information Processing Systems (NEURIPS)*, S. Koyejo, S. Mohamed, A. Agarwal, D. Belgrave, K. Cho, and A. Oh (Eds.), Vol. 35. MIT Press, Cambridge, MA, 507–520.

[17] Suryabhan Singh Hada and Miguel Á. Carreira-Perpiñán. 2021. Exploring Counterfactual Explanations for Classification and Regression trees. In *ECML PKDD 3rd Int. Workshop and Tutorial on eXplainable Knowledge Discovery in Data Mining (XKDD 2021)*. 489–504.

[18] Trevor J. Hastie and Robert J. Tibshirani. 1990. *Generalized Additive Models.* Number 43 in Monographs on Statistics and Applied Probability. Chapman & Hall, London, New York.

[19] Trevor J. Hastie, Robert J. Tibshirani, and Jerome H. Friedman. 2009. *The Elements of Statistical Learning—Data Mining, Inference and Prediction* (second ed.). Springer-Verlag.

[20] Guolin Ke, Qi Meng, Thomas Finley, Taifeng Wang, Wei Chen, Weidong Ma, Qiwei Ye, and Tie-Yan Liu. 2017. LightGBM: A Highly Efficient Gradient Boosting Decision Tree. In *Advances in Neural Information Processing Systems (NIPS)*, I. Guyon, U. v. Luxburg, S. Bengio, H. Wallach, R. Fergus, S. Vishwanathan, and R. Garnett (Eds.), Vol. 30. MIT Press, Cambridge, MA, 3146–3154.

[21] M. Lichman. 2013. UCI Machine Learning Repository. http://archive.ics.uci.edu/ml.

[22] Wei-Yin Loh. 2002. Regression Trees with Unbiased Variable Selection and Interaction Detection. *Statistica Sinica* 12, 2 (April 2002), 361–386.

[23] Yin Lou, Rich Caruana, Johannes Gehrke, and Giles Hooker. 2013. Accurate Intelligible Models with Pairwise Interactions. In *Proc. of the 19th ACM SIGKDD Int. Conf. Knowledge Discovery and Data Mining (SIGKDD 2013)*. Chicago, IL, 623–631.

[24] David Lubinsky. 1994. Classification Trees with Bivariate Splits. *Applied Intelligence* 4, 3 (July 1994), 283–296.

[25] S. K. Murthy, S. Kasif, and S. Salzberg. 1994. A System for Induction of Oblique Decision Trees. *J. Artificial Intelligence Research* 2 (1994), 1–32.

[26] Sreerama K. Murthy, Simon Kasif, Steven Salzberg, and Richard Beigel. 1993. OC1: A Randomized Algorithm for Building Oblique Decision Trees. In *Proc. of the 11th AAAI Conference on Artificial Intelligence (AAAI 1993)*. Washington, DC, 322–327.

[27] Nina Narodytska, Alexey Ignatiev, Filipe Pereira, and Joao Marques-Silva. 2003. Learning Optimal Decision Trees with SAT. In *Proc. of the 18th Int. Joint Conf. Artificial Intelligence (IJCAI'03)*. Acapulco, Mexico, 1362–1368.

[28] Siegfried Nijssen and Elisa Fromont. 2010. Optimal Constraint-Based Decision Tree Induction from Itemset Lattices. *Data Mining and Knowledge Discovery* 21, 1 (July 2010), 9–51.

[29] Tim Oates and David Jensen. 1997. The Effects of Training Set Size on Decision Tree Complexity. In *Proc. of the 14th Int. Conf. Machine Learning (ICML'97)*, D. H. Fisher (Ed.). Nashville, TN, 254–262.

[30] Fabian Pedregosa, Gaël Varoquaux, Alexandre Gramfort, Vincent Michel, Bertrand Thirion, Olivier Grisel, Mathieu Blondel, Peter Prettenhofer, Ron Weiss, Vincent Dubourg, Jake Vanderplas, Alexandre Passos, David Cournapeau, Matthieu Brucher, Matthieu Perrot, and Édouard Duchesnay. 2011. Scikit-learn: Machine Learning in Python. *J. Machine Learning Research* 12 (Oct. 2011), 2825–2830. Available online at https://scikit-learn.org.

[31] J. Ross Quinlan. 1993. *C4.5: Programs for Machine Learning*. Morgan Kaufmann.

[32] Steffen Rendle. 2010. Factorization Machines. In *Proc. of the 10th IEEE Int. Conf. Data Mining (ICDM 2010)*. Sydney, Australia, 995–1000.

[33] Lior Rokach and Oded Maimon. 2015. *Data Mining With Decision Trees. Theory and Applications* (second ed.). Number 81 in Series in Machine Perception and Artificial Intelligence. World Scientific.

[34] Sicco Verwer and Yingqian Zhang. 2019. Learning Optimal Classification Trees Using a Binary Linear Program Formulation. In *Proc. of the 33rd AAAI Conference on Artificial Intelligence (AAAI 2019)*. Honolulu, HI, 1625–1632.

[35] Arman Zharmagambetov and Miguel Á. Carreira-Perpiñán. 2020. Smaller, More Accurate Regression Forests Using Tree Alternating Optimization. In *Proc. of the 37th Int. Conf. Machine Learning (ICML 2020)*, Hal Daumé III and Aarti Singh (Eds.). Online, 11398–11408.

[36] Arman Zharmagambetov and Miguel Á. Carreira-Perpiñán. 2022. Learning Interpretable, Tree-Based Projection Mappings for Nonlinear Embeddings. In *Proc. of the 25th Int. Conf. Artificial Intelligence and Statistics (AISTATS 2022)*. Online, 9550–9570.

[37] Arman Zharmagambetov and Miguel Á. Carreira-Perpiñán. 2022. Semi-Supervised Learning with Decision Trees: Graph Laplacian Tree Alternating Optimization. In *Advances in Neural Information Processing Systems (NEURIPS)*, S. Koyejo, S. Mohamed, A. Agarwal, D. Belgrave, K. Cho, and A. Oh (Eds.), Vol. 35. MIT Press, Cambridge, MA, 2392–2405.

[38] Arman Zharmagambetov, Suryabhan Singh Hada, Magzhan Gabidolla, and Miguel Á. Carreira-Perpiñán. 2021. Non-Greedy Algorithms for Decision Tree Optimization: An Experimental Comparison. In *Int. J. Conf. Neural Networks (IJCNN'21)*. Virtual event.

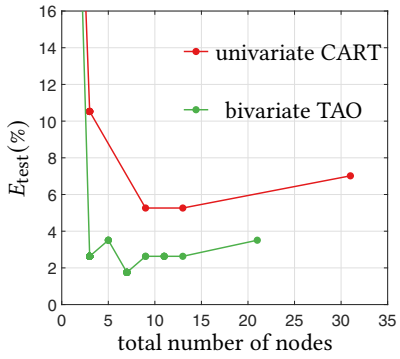

Figure 9: Test error (on the Breast Cancer dataset) of univariate CART and bivariate TAO trees as a function of the number of nodes (obtained from the regularization path over their hyperparameter).

Table 3: Comparison between bivariate, univariate and oblique trees for classification. Each tree was selected by cross-validating its hyperparameter and this was repeated 3 times over random training/validation sets. We report training and test accuracy (% ±stdev); average depth Δ, node count n and number of features f per node (we omit $f = 1$ and 2 for univariate and bivariate trees, respectively); and average runtime (seconds or "timeout"). We indicate with color green best and blue second best result for test accuracy and node count over the univariate and bivariate trees (ignoring the oblique trees).

Dataset	(N_{train}, D, K)		bivariate			univariate		oblique
			TAO	CART	BiDT	CART	C5.0	TAO
Breast Cancer	(455,30, 2)	training (%)	96.04±1.53	99.12±0.00	96.99±0.10	98.61±0.41	98.9±0.48	98.21±0.79
		test (%)	98.25±0.43	98.00±0.00	97.66±0.10	94.73±0.00	95.6±0.67	97.71±1.04
		Δ/#nodes/f	1/3	3.0/9	1.6/5	4.0/16	5.3/12	3/15/10.3
		runtime (s)	4	6	2	0.1	0.1	5
Segment	(1963,19, 7)	training (%)	98.47±0.35	97.30±0.00	97.58±0.01	98.76±0.00	98.9±0.10	99.48±0.21
		test (%)	97.41±0.14	96.73±0.14	96.06±0.14	96.01±0.47	96.3±0.48	97.58±1.31
		Δ/#nodes/f	11.0/13	11.0/25	9.0/21	15.0/128	12.25/77	8/271/8.5
		runtime (s)	30	13	27	0.1	0.1	20
Optical recog.	(3823,62,10)	training (%)	97.28±0.36	97.65±0.01	98.70±0.50	98.32±1.18	98.5±0.18	97.68±0.59
		test (%)	88.48±0.39	87.03±0.02	88.10±0.32	85.32±0.22	86.8±0.23	91.27±1.74
		Δ/#nodes/f	9.0/54	14.0/149	16.0/188	15.0/358	13.65/335	7/115.8/15.0
		runtime (s)	30	233	17	0.3	0.3	10
Spambase	(3910,57, 2)	training (%)	96.39±0.08	97.49±0.14	95.34±1.85	97.86±2.91	96.16±0.14	96.55±0.47
		test (%)	93.34±0.07	92.19±0.05	92.71±0.53	92.18±0.31	92.2±0.42	94.31±1.22
		Δ/#nodes/f	14/53	10.0/77	16/161	24.7/362	14.7/77	4/30/42.1
		runtime (s)	120	284	208	0.3	0.3	60
Pageblock	(4652,10, 5)	training (%)	98.39±0.00	98.41±0.00	99.19±0.40	99.74±0.01	97.7±0.09	95.96±0.12
		test (%)	97.93±00	96.83±0.01	96.38±0.06	96.52±0.17	96.54±0.13	96.35±0.41
		Δ/#nodes/f	8.0/25	18.0/159	4.3/14	18/268	10.05/90	6/39/7.5
		runtime (s)	30	21	15	0.2	0.1	39
House 16H	(11464,16, 2)	training (%)	87.1±1.55	89.45±0.00	90.42±0.23	86.2±0.0	91.98±0.55	86.55±1.10
		test (%)	85.6±0.07	84.73±0.05	85.6±0.17	83.4±0.0	83.06±0.32	85.47±0.51
		Δ/#nodes/f	7/35	10/107	10/115	8/75	15.05/245	4/13/14.9
		runtime (s)	30	21	15	0.2	0.1	24
Letter	(16000,16,26)	training (%)	100±1.37	100±0.01	98.40±1.76	94.30±0.01	98.66±0.07	95.43±0.29
		test (%)	87.25±0.11	87.25±0.00	86.80±0.37	86.04±0.04	86.76±0.33	90.41±0.31
		Δ/#nodes/f	35/1314	35.0/2121	37.6/2596	28/3888	16.85/2817	11/2155/8.5
		runtime (s)	300	73	12*	0.3	0.9	77
Electricity	(32702, 8, 2)	training (%)	98.97±2.80	95.80±0.80	96.14±1.20	99.10±0.00	95.04±0.43	98.1±1.8
		test (%)	89.38±0.12	86.05±0.05	87.91±0.06	87.80±0.16	88.64±0.42	90.23±0.19
		Δ/#nodes/f	23.0/1083	24.0/1741	22.3/1881	30.0/6366	17.25/2615	10/249/6.8
		runtime (s)	300	81	393	0.9	0.9	134
MiniBooNE	(62048,50, 2)	training (%)	92.36±0.00	96.02±0.02	-	96.61±0.02	95.88±0.07	91.98±0.15
		test (%)	91.16±0.00	90.68±0.03	-	90.25±0.03	89.84±0.10	91.43±0.12
		Δ/#nodes/f	11.0/105	15/831	-	19.3/2012	15.65/1787	10/133/16.8
		runtime (s)	1200	1000	timeout	5.2	6.4	3000
SUSY	(600000,18, 2)	training (%)	80.71±0.00	81.35±0.00	-	81.45±0.00	80.90±0.00	81.10±0.00
		test (%)	79.51±0.00	79.01±0.00	-	78.90±0.00	79.10±0.00	80.3±0.00
		Δ/#nodes/f	17.0/1077	21/2780	-	24/4389	16.25/3227	12/983
		runtime (s)	≈2h	≈1h	timeout	40.2	35.2	≈2h

A Experiment setup

We use the CART Python implementation in `scikit-learn` [30]. We grow the tree to its maximum depth by setting the `minsplit` parameter to 1 and the `ccp alpha` complexity parameter to 0, and determine the optimal pruning parameter on the hold-out set.

We employ an open-source single-threaded Linux version of the C5.0 implementation in C (https://rulequest.com/download.html). To optimize model performance for each dataset, we conduct a grid search on the hold-out set to identify the most suitable parameters. We mainly fine-tune two parameters: `-c CF`, which governs the pruning severity, and `-m cases`, which specifies the minimum number of data points required to split a node. It's worth noting that we maintain default configurations for all other model parameters. Remarkably, our findings indicate that the tuned parameter values closely align with the default settings in many instances.

We use an open-source multithreaded implementation of BiDT by [3] written in C++ with Python interface (https://github.com/fbollwein/OptimizedDecisionTrees). We enable both univariate and bivariate splits. The resulting tree grows fully and is then pruned either using reduced error pruning or minimum cost-complexity pruning using the hold-out set.

We implement bivariate TAO in C++ with parallel processing and fine-tune regularization parameters C and λ. For each experiment we start with $C = 1$ and increase in with a step of 0.25 until the tree becomes fully univariate. Through empirical analysis, it was found that algorithm generalizes well when C falls within the

Table 5: Feature description of Segment dataset. Description provided from the official UCI web page. Index column is used to indicate features in fig. 8 in the main paper.

Index	Description
x_0	the column of the center pixel of the region
x_1	the row of the center pixel of the region
x_2	# pixels in a region = 9
x_3	# lines of low contrast that go through the region
x_4	# lines of high contrast, greater than 5
x_5	contrast of horizontally adjacent pixels in the region
x_6	standard deviation of prev. feature
x_7	contrast of vertically adjacent pixels
x_8	standard deviation of prev. feature
x_9	average over the region of (R + G + B)/3
x_{10}	average over the region of the R
x_{11}	average over the region of the B
x_{12}	average over the region of the G
x_{13}	excess red: (2R - (G + B))
x_{14}	excess blue: (2B - (G + R))
x_{15}	excess green: (2G - (R + B))
x_{16}	Value of HSV
x_{17}	Saturation of HSV
x_{18}	Hue of HSV

Table 6: Comparison between bivariate CART and univariate CART initialization for bivariate TAO. We report train and test accuracy (%, ±stdev over 3 runs), average depth Δ of the tree and average node count.

Dataset	(N_{train}, D, K)		bivariate CART init.	univariate CART init.
Breast Cancer	(455,30, 2)	training (%)	96.04±1.53	99.12±0.01
		test (%)	98.25±0.43	97.37±0.12
		Δ/#nodes	1/3	3.1/9.5
Segment	(1963,19, 7)	training (%)	98.47±0.35	99.03±0.30
		test (%)	97.41±0.14	97.12±1.10
		Δ/#nodes	11.0/13	12.0/45.3
Optical recog.	(3823,62,10)	training (%)	97.28±0.36	97.17±0.05
		test (%)	88.48±0.39	87.65±0.11
		Δ/#nodes	14.0/61	11.0/123
Spambase	(3910,57, 2)	training (%)	96.78±0.08	96.39±0.08
		test (%)	92.32±0.07	93.34±0.07
		Δ/#nodes	11/28	14.0/53
Pageblock	(4652,10, 5)	training (%)	98.39±0.00	98.24±0.01
		test (%)	97.93±00	97.81±0.01
		Δ/#nodes	8.0/25	5.0/23
House 16H	(11464,16, 2)	training (%)	91.42±1.55	87.1±1.55
		test (%)	84.93±0.07	85.6±0.07
		Δ/#nodes	11/83	7/35
Letter	(16000,16,26)	training (%)	98.3±1.37	97.25±1.37
		test (%)	87.25±0.11	86.99±0.11
		Δ/#nodes	35/1314	28/2005
Electricity	(32702, 8, 2)	training (%)	98.97±2.80	96.80±0.80
		test (%)	89.38±0.12	87.05±0.05
		Δ/#nodes	23.0/1083	24.0/1141
MiniBooNE	(62048,50, 2)	training (%)	94.72±0.00	92.36±0.00
		test (%)	91.31±0.00	91.16±0.00
		Δ/#nodes	13.0/225	11/105

Table 4: List of features of Breast Cancer dataset. Description provided from the official UCI web page. Index column is used to indicate features in fig. 7 in the main paper.

radius1	radius2	radius3
texture1	texture2	texture3
perimeter1	perimeter2	perimeter3
area1	area2	area3
smoothness1	smoothness2	smoothness3
compactness1	compactness2	compactness3
concavity1	concavity2	concavity3
concave points1	concave points2	concave points3
symmetry1	symmetry2	symmetry3
fractal dimension1	fractal dimension2	fractal dimension3

range of 1 and 2.5 across most datasets. Since running algorithm for each value of λ is computationally costly we perform coarse search with finer steps closer to 0. As it was discussed in section 3.2 in the main paper, every next value of λ can be calculated for given C. We generate a fixed subset of line inclinations H uniformly between 0 and 180 degrees and for most experiments H is set between 30 and 90. We use save values of H for bivariate CART. The initial tree structure is obtained from fully grown CART tree (univariate or bivariate).

We run our experiments on datasets from UCI ML repository [21] and [16]. For datasets that does not have separate test set we randomly subsample 20% of the whole dataset for testing. We randomly select 10% of samples as hold-out set for validation. For experiments, we report average over 3 runs with stdev for train and test accuracy. We set a timeout of 2 hours for all algorithms on all datasets except for SUSY (≈600k samples), for which it was increased to 4 hours. Our hardware setup is Intel Xeon CPU E5-2699 v3 @ 2.30GHz with 256 GB RAM.

B Additional experimental results

Table 6 presents results of different initialization for bivariate TAO. We use initial tree structure produced by univariate and bivariate CART proposed in section 3.4. Initializing from bivariate CART generally results in smaller and better performing final trees. In the main paper we use both initializations and pick the best one on the validation set.